



HAL
open science

Surface-induced spin state locking of the [Fe(H₂B(pz)₂)₂(bipy)] spin crossover complex

Sumit Beniwal, X. Zhang, Sai Mu, Ahmad Naim, Patrick Rosa, Guillaume Chastanet, Jean-François Létard, J. Liu, George E. Sterbinsky, Dario A. Arena, et al.

► **To cite this version:**

Sumit Beniwal, X. Zhang, Sai Mu, Ahmad Naim, Patrick Rosa, et al.. Surface-induced spin state locking of the [Fe(H₂B(pz)₂)₂(bipy)] spin crossover complex. *Journal of Physics: Condensed Matter*, 2016, 28 (20), pp.206002. 10.1088/0953-8984/28/20/206002 . hal-01314476

HAL Id: hal-01314476

<https://hal.science/hal-01314476v1>

Submitted on 27 Jan 2021

HAL is a multi-disciplinary open access archive for the deposit and dissemination of scientific research documents, whether they are published or not. The documents may come from teaching and research institutions in France or abroad, or from public or private research centers.

L'archive ouverte pluridisciplinaire **HAL**, est destinée au dépôt et à la diffusion de documents scientifiques de niveau recherche, publiés ou non, émanant des établissements d'enseignement et de recherche français ou étrangers, des laboratoires publics ou privés.

Spin state locking of Fe(II) spin crossover complex

Switching-induced spin state locking of the $[\text{Fe}(\text{H}_2\text{B}(\text{pz})_2)_2(\text{bipy})]$ spin crossover complex

S Beniwal,^{1,5} X Zhang,^{1,5} S Mu,¹ A Naim,² P Rosa,² G Chastanet,² J-F Létard,² J Liu,^{3,4} G E Sterbinsky,⁴ D A Arena,⁴ P A Dowben,¹ and A Enders^{1*}

¹ Department of Physics and Astronomy, University of Nebraska – Lincoln, Lincoln, NE, USA, 68588.

² CNRS, Université de Bordeaux, ICMCB, UPR 9048, 87 avenue du Dr. A. Schweitzer, Pessac, F-33608, France.

³ Department of Chemical Engineering, Northeastern University, Boston, MA, U.S.A.

⁴ National Synchrotron Light Source, Brookhaven National Laboratory, Upton, NY, U.S.A.

⁵ These authors contributed equally.

Email: a.enders@me.com

Temperature- and coverage-dependent studies of the Au(111)-supported spin crossover Fe(II) complex (SCO) of the type $[\text{Fe}(\text{H}_2\text{B}(\text{pz})_2)_2(\text{bipy})]$ with a suite of surface-sensitive spectroscopy and microscopy tools show that the substrate inhibits thermally induced transitions of the molecular spin state, so that both high-spin and low-spin states are preserved far beyond the spin transition temperature of free molecules. Scanning tunneling microscopy confirms that $[\text{Fe}(\text{H}_2\text{B}(\text{pz})_2)_2(\text{bipy})]$ grows as ordered, molecular bilayer islands at sub-monolayer coverage and as disordered film at higher coverage. The temperature dependence of the electronic structure suggest that the SCO films exhibit a mixture of spin states at room temperature, but upon cooling below the spin crossover transition the film spin state is best described as a mix of high-spin and low-spin state molecules of a ratio that is constant. This locking of the spin state is most likely the result of a substrate-induced conformational change of the interfacial molecules, but it is estimated that also the intra-atomic electron-electron Coulomb correlation energy, or Hubbard correlation energy U , could be an additional contributing factor.

Keywords: spin-crossover, Fe(II) spin-crossover, molecular magnetism, spin state locking

PACS: 75.30.Wx; 68.37Ef; 68.43Fg; 79.60.Dp

Submitted to: Journal of Physics: Condensed Matter

1. Introduction

Molecules with switchable magnetic moment, such as Fe(II) complexes of pseudo-octahedral geometry, are interesting and promising candidate materials for the emerging field of organic spintronics [1-7]. The molecules' outstanding and useful physical property is that their central Fe(II) atom can exist in either a high spin (HS) or a low spin (LS) magnetic state, derived from the possible electronic configurations of t_{2g}^6 (LS) or $t_{2g}^4e_g^2$ (HS). A reversible spin crossover (SCO) transition between HS and LS states can be induced by external stimuli such as temperature [1-7], pressure [8], electric field [9] and by light [10,11]. The switching of the spin state is strongly dependent of the local environment of the Fe ion, which is susceptible to crystal packing and the presence of an extraneous matrix, and can

also be affected by long-range effects such as cooperativity between adjacent molecules [1,4,12-15]. When considering molecules deposited on top of a surface, the influence of the substrate cannot be discounted as it has been compellingly demonstrated [9,16-18].

While the SCO transition of modestly thick supported films can be similar to that of powders [19], studies done on various Fe(II) complexes do show that the HS-LS transition can change considerably with respect to the bulk behavior when prepared as a monolayer or submonolayer thin film on a substrate surface [9,16-18]. The substrate thus becomes an important parameter to alter the SCO behavior by manipulating the transition temperature and the cooperativity between molecules. For instance, Miyamachi *et al.* [17] showed that a HS-

Spin state locking of Fe(II) spin crossover complex

LS transition cannot be induced by a local electric field in $[\text{Fe}(\text{phen})_2(\text{NCS})_2]$ molecules (phen=1,10-phenanthroline) on Cu(100) at 5 K, but that a reversible switching is possible on CuN/Cu(100). Similarly, Gopakumar *et al.* [16] found that the spin state of $[\text{Fe}(\text{H}_2\text{B}(\text{pz})_2)_2\text{phen}]$ molecules ($\text{H}_2\text{B}(\text{pz})_2$ =bis(hydrido)-bis-(1*H*-pyrazol-1-yl)borate) in single monolayers on Au(111) appears to be locked in, while molecules in a second layer can be reversibly switched between HS and LS states using the electric field from the tip of a scanning tunneling microscope (STM).

X-ray absorption spectroscopy (XAS) is a powerful experimental technique to probe the spin states of supported SCO molecules on various substrates, where characteristic changes in the line shape at the Fe L_3 and L_2 absorption edge, as a function of temperature, can be used to monitor the interconversion between HS and LS states. Using XAS, the HS and LS states for $[\text{Fe}(\text{H}_2\text{B}(\text{pz})_2)_2(\text{phen})]$ [16], $[\text{Fe}(\text{phen})_2(\text{NCS})_2]$ [17], and $[\text{Fe}(\text{H}_2\text{B}(\text{pz})_2)_2(\text{bipy})]$ (bipy=2,2'-bipyridine) [18] have been shown to coexist across a wide range of temperatures for supported ultrathin films. These studies evidenced that the proportion of HS and LS occupancy varies with temperature for thin films. STM results for $[\text{Fe}(\text{phen})_2(\text{NCS})_2]$ suggest that the conducting substrate has a significant influence on the SCO transition [17], and there seems to be general consensus that a conducting substrate will tend to pin more than 50% of several SCO complexes in the high spin state even well below the SCO transition temperature [16,18]. While it is clear that coordination effects and cooperativity of SCO complexes are critically dependent on the substrate, detailed knowledge of fundamental interactions at the molecule-substrate interface and how they can be exploited to control the spin crossover effect, needs to be established through basic research before those materials can be considered for organic spintronics applications.

We have shown in earlier studies that organic molecules in contact with crystalline surfaces generally can experience considerable changes in their conformation [20], energy level realignment, charge transfer, and a decrease in their dipole moment [21,22], emphasizing the impact of interface interactions on adsorbate molecule properties. In this article we demonstrate how the spin state of SCO molecules is affected by a supporting substrate. We will present studies of the temperature and thickness dependence of the SCO complex $[\text{Fe}(\text{H}_2\text{B}(\text{pz})_2)_2(\text{bipy})]$ on Au(111) with a comprehensive suite of surface-sensitive

spectroscopy and microscopy tools, which show that the substrate not only inhibits thermal transition of the molecular spin state, it preserves each spin state far beyond the transition temperature of free molecules.

2. Experimental and Computational Details

The $[\text{Fe}(\text{H}_2\text{B}(\text{pz})_2)_2(\text{bipy})]$ complex was synthesized as described previously [23]. The thermal SCO transition for the powder is determined to be in agreement with previous results [19,23]. Molecular thin films were deposited for these studies with home built Knudsen-like molecular evaporator on a single crystal Au(111) substrate held at room temperature. Scanning tunneling microscopy was carried out in two different Omicron STM systems at 77 K and at room temperature. X-ray photoemission spectra (XPS) and angle-dependent XPS spectra were obtained using non-monochromatized Al $K\alpha$ x-ray source, with a photo energy of 1486.6 eV, and a SPECS PHOIBOS 150 energy analyzer. The core level binding energies were calibrated to a gold reference, with the Au $4f_{7/2}$ core level peak placed at 84 eV, all at room temperature. The CasaXPS software was used to analyze the X-ray photoemission core level spectra [24] and a Shirley-type background was subtracted to obtain X-ray photoemission core level spectra peak areas [25,26]. STM and XPS measurements were performed in-situ immediately following the sample growth in UHV.

X-ray absorption spectroscopy (XAS) measurements of $[\text{Fe}(\text{H}_2\text{B}(\text{pz})_2)_2(\text{bipy})]$ thin films and powder were performed at the U4B beamline at the National Synchrotron Light Source of Brookhaven National Laboratory [27]. The measurements were taken in the total electron yield mode of operation across the Fe $2p_{3/2}$ or L_3 edge and Fe $2p_{1/2}$ or L_2 edge. The collected spectra were normalized by the incident beam intensity, which was monitored by a Au mesh mounted upstream of the sample chamber. The Fe $L_{3,2}$ edge spectrum of an iron oxide (Fe_2O_3) film was measured as an accompaniment to the XAS data for each molecular complex sample as reference for alignment and calibration.

First-principles calculations were carried out using projected augmented wave method (PAW) [28] and density functional theory (DFT) as implemented in the Vienna *ab initio* simulation package (VASP) [29,30]. We used the plane-wave energy cutoff of 500 eV and the Γ point for the Brillouin zone integration. We embedded a single

Spin state locking of Fe(II) spin crossover complex

[Fe(H₂B(pz)₂)₂(bipy)] molecule, whose structure is taken from the experiment [31], into a 50×50×50 Å³ cubic unit cell, and performed calculations for the electronic structure, particularly for the weights of unoccupied *e_g* and *t_{2g}* states. The positions of H atoms were optimized by DFT in the ground state. Gaussian smearing of 0.1 eV was adopted for the static calculations. Both HS state and LS state were obtained to confirm the ground state for the [Fe(H₂B(pz)₂)₂(bipy)] molecules. To describe the electronic structure correctly, we used the rotationally invariant local density approximation (LDA)+*U* method [32] without LSDA exchange splitting. For the Fe based SCO complex under consideration, in the low spin state, the six 3*d* electrons are paired and occupy the three *t_{2g}*-like orbitals leaving the *e_g*-like orbitals empty, in the crystal field picture. In the high spin state, the *e_g* set is filled with two unpaired electrons while four electrons occupy the three orbitals of the *t_{2g}*. The usually degenerate *t_{2g}* and *e_g* subset can be split into multiple levels by deviations of molecular geometry from perfectly octahedral. Since the orbital dependent potential relies on the choice of Hubbard correlation *U*, the orbital occupation values are *U*-dependent as well. Therefore, it is of some importance to consider the Hubbard correlation *U* dependence of the *e_g*/*t_{2g}* ratios in both LS and HS states.

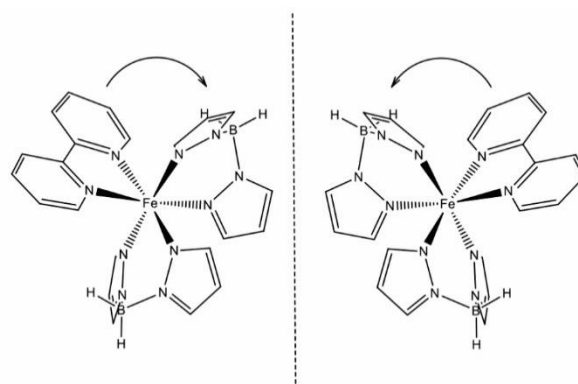
3. Results and Discussion

3.1 Structure and morphology of SCO complex layers

STM images of [Fe(H₂B(pz)₂)₂(bipy)] on Au(111) are shown in figure 1. The molecules are highly mobile across the Au surface at room temperature for sub-monolayer coverage, and move considerably faster than the typical line capture time of our STM. As a result, the well-known herringbone reconstruction of the Au(111) surface is visible, superimposed by streaks caused by diffusing adsorbate molecules (figure 1(a)). The presence of molecules on this sample is, nonetheless, evident from XPS Fe 2p core level spectra.

The [Fe(H₂B(pz)₂)₂(bipy)] molecules condense partly into ordered double-layer islands upon cooling the sample to 77 K, as seen in figure 1(b), but a significant portion of the molecules remains as a surface gas or dilute fluid between the condensed islands. Higher magnification STM images, showing structural details of the condensed islands, are presented in figure 1(c) and (d). A structural

model of this [Fe(H₂B(pz)₂)₂(bipy)] double layer has been established in earlier work by Pronschinske *et al.* [33], based on a model proposed in a previous work by Gopakumar *et al.* [34] for the closely related [Fe(H₂B(pz)₂)₂(phen)] complex. Not considered in those models is that these related SCO complexes are actually non-centrosymmetric, and exist in right- and left-handed configurations, depicted in scheme 1 for [Fe(H₂B(pz)₂)₂(bipy)]. Those models should lead to structural domains that are mirror images in the plane of the surface, which would be symptomatic of some chiral segregation effected by the surface acting as chiral discriminant, but such segregation was not observed in this and previous works.



Scheme 1. Right-handed and left-handed configurations of the non-centrosymmetric [Fe(H₂B(pz)₂)₂(bipy)] complex.

This leads us to conclude that the two configurations are present in the crystal structure as a racemic mix. Each [Fe(H₂B(pz)₂)₂(bipy)] molecule in the top layer appears as a three-lobe structure, as is seen in the magnified area in figure 1(d). Two lobes were identified in the previous models [33,34] as pyrazole ligands, and the third lobe is the pyridine ligand, which appears slightly darker than the pyrazole lobes in the STM images. The [Fe(H₂B(pz)₂)₂(bipy)] molecules appear to be arranged along rows, where molecules in adjacent rows are seemingly rotated by 70 degrees with respect to one another (as shown by the colored triangles in figure 1(d)), as the result of their stacking on top of the molecular layer underneath. Since this simple rotation leads to the same handedness and an overall isochiral domain, the possibility that adjacent rows correspond to opposite handedness should be considered, leading thus to a racemic paving of the surface.

Spin state locking of Fe(II) spin crossover complex

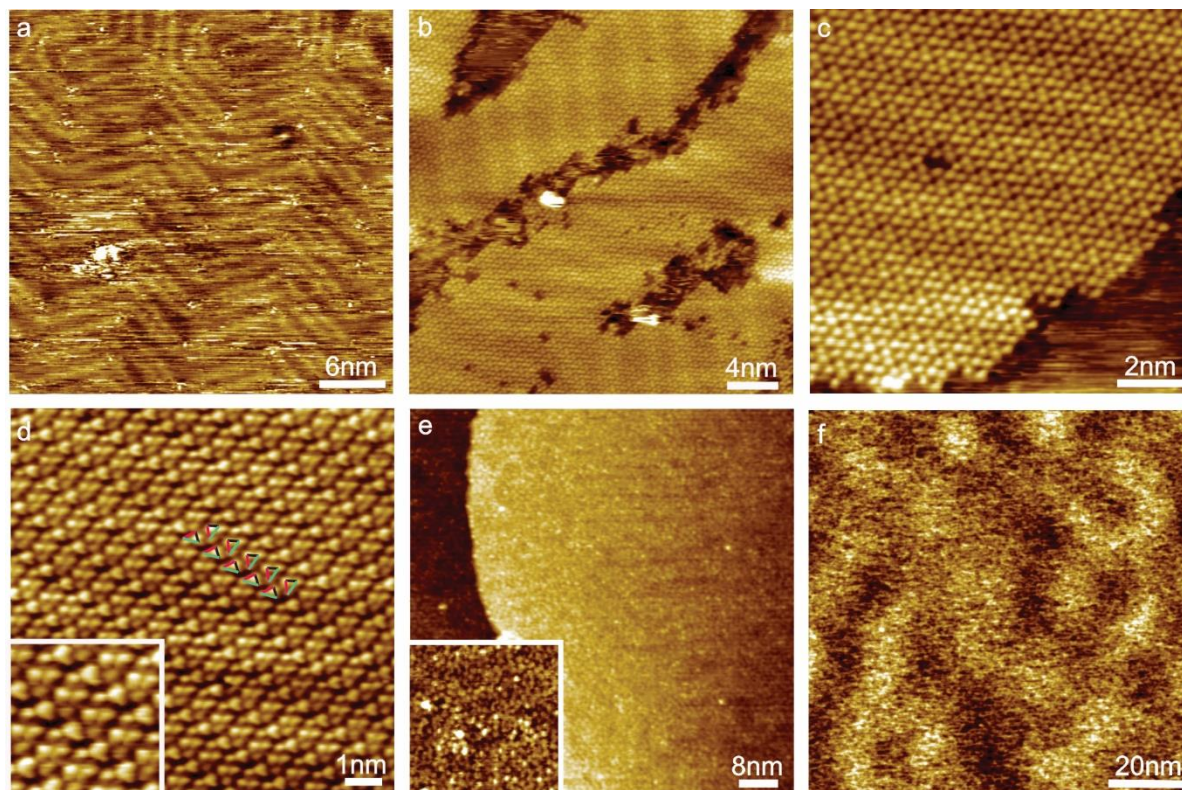


Figure 1. Scanning Tunneling Microscopy images of different $[\text{Fe}(\text{H}_2\text{B}(\text{pz})_2)_2(\text{bipy})]$ film thicknesses on Au(111) (a) sub-monolayer coverage at room temperature, $I_t = 0.3 \text{ nA}$, $V_b = -0.5 \text{ V}$, (b) Bilayer islands of $[\text{Fe}(\text{H}_2\text{B}(\text{pz})_2)_2(\text{bipy})]$ at 77 K, $I_t = 1 \text{ nA}$, $V_b = -1 \text{ V}$, (c) sub-molecular resolution of bilayer islands at 77 K, $I_t = 0.5 \text{ nA}$, $V_b = -1 \text{ V}$, (d) alternate rows appear different at different bias voltage, $I_t = 1 \text{ nA}$, $V_b = -0.2 \text{ V}$ (e) 7 ± 3 monolayer thick film of $[\text{Fe}(\text{H}_2\text{B}(\text{pz})_2)_2(\text{bipy})]$ at room temperature, $I_t = 0.4 \text{ nA}$, $V_b = -0.8 \text{ V}$, (f) non-contact AFM images of 25 ± 5 monolayer thick film of $[\text{Fe}(\text{H}_2\text{B}(\text{pz})_2)_2(\text{bipy})]$ at room temperature.

Increasing the $[\text{Fe}(\text{H}_2\text{B}(\text{pz})_2)_2(\text{bipy})]$ molecular coverage results in a molecular film which appears to be disordered, as seen in figure 1(e). This disorder builds into the condensed film for surprisingly thin films of just a few monolayers, so the exact film thickness is obscured by the degree of disorder. Yet the visibility of the Au(111) reconstruction, through the disordered films, somewhat thicker than the molecular bilayer, suggests strongly that the film is not thicker than a few monolayers (7 ± 3).

$[\text{Fe}(\text{H}_2\text{B}(\text{pz})_2)_2(\text{bipy})]$ is a dielectric [19], as is evident in the increase of binding energy for the Fe $2p_{3/2}$ core level from $706.5 \pm 0.3 \text{ eV}$ to 710 eV [19] and to 711.5 eV [33] for thicker films as a result of either decreased substrate screening or final state charging. Conductance measurements performed on small single crystals evidence a resistivity consistently higher than $10 \text{ G}\Omega$ in the temperature range between 4 and 300 K. Consistent with this

picture of $[\text{Fe}(\text{H}_2\text{B}(\text{pz})_2)_2(\text{bipy})]$ as a dielectric, thicker films of several nanometers thickness, could not be imaged with STM. Atomic force microscopy (AFM) does provide indications that the thicker $[\text{Fe}(\text{H}_2\text{B}(\text{pz})_2)_2(\text{bipy})]$ film morphology remains fairly flat so that for a nominally 25 ± 5 monolayer thick films of $[\text{Fe}(\text{H}_2\text{B}(\text{pz})_2)_2(\text{bipy})]$, we find an RMS roughness of 0.7 nm , or about the diameter of a molecule (figure 1(f)).

3.2 Electronic configuration

The electronic structure of the $[\text{Fe}(\text{H}_2\text{B}(\text{pz})_2)_2(\text{bipy})]$ films as a function of their thicknesses were studied using XPS. The thickness of all films was estimated from the intensity ratio of substrate and adsorbate XPS peak intensities, as the films appear disordered in STM and AFM (as discussed above). The XPS Fe $2p$ core level spectra obtained from three films of different thickness at

Spin state locking of Fe(II) spin crossover complex

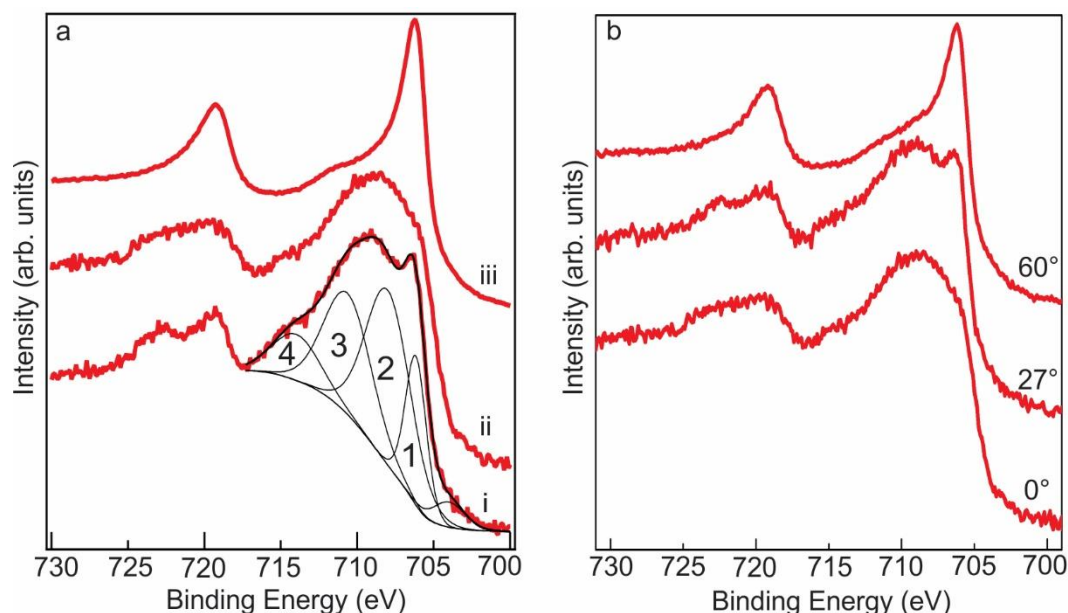


Figure 2. X-ray photoemission of the Fe 2p core level for increasing $[\text{Fe}(\text{H}_2\text{B}(\text{pz})_2)_2(\text{bipy})]$ film thicknesses on Au(111) (a) (i) A bilayer coverage at room temperature, corresponding to figure 1d (ii) 7 ± 3 monolayer thick film at room temperature corresponding to figure 1(e) (iii) A thicker film of 25 ± 5 monolayers (b) Angular dependent XPS for 7 ± 3 monolayer film.

room temperature are shown in figure 2(a). For a bilayer film, the XPS spectra exhibit broad Fe $2p_{3/2}$ and Fe $2p_{1/2}$ peaks. These broad core level features are the result of peak splitting and the appearance of one or more shake-up satellites. The splitting of the $2p_{3/2}$ core level feature disappears with increasing $[\text{Fe}(\text{H}_2\text{B}(\text{pz})_2)_2(\text{bipy})]$ film thickness. Peak fitting that considers a split $2p_{3/2}$ peak and two shake-up satellites have been performed with a pre-peak, as demonstrated on the example of the bilayer film spectra in figure 2(a)(i) [35-38]. Although of decreasing intensity, the principal satellite features persists over a considerable range of film thickness. At coverage of approximately 25 ± 5 monolayers (figure 2(a)(iii)), the XPS spectra are similar to those obtained from powder and thicker films, exhibiting sharp $2p_{3/2}$ and $2p_{1/2}$ peaks and comparably small shoulder features or shake-up satellites. However, the binding energy for the Fe $2p_{3/2}$ core level is found to be 706.5 ± 0.3 eV as opposed to earlier published energies of 710 eV [19] and 711.5 eV [33]. The Fe 2p XPS for UHV imprinted film on Au(111) is shown in the figure S1 in supplementary information (ESI). The shake-up satellite peaks at higher binding energies can be due to a number of effects, such as multiplet splitting or ligand metal charge transfer. The satellite peaks

were certainly seen in the XPS spectra of thicker $[\text{Fe}(\text{H}_2\text{B}(\text{pz})_2)_2(\text{bipy})]$ films [33] in the high-spin state, but the satellite intensities here are far larger than previously reported [9, 33, 39, 42, 43]. So is it possible that the strong satellite features are the result of a mixture of Fe^{3+} and Fe^{2+} , as there is some resemblance to the Fe $2p$ spectra in prior work [38, 44-46]? This is very unlikely: A mixture of Fe^{3+} and Fe^{2+} would require a significant change in Fe 3d occupancy. We investigated the Fe 3d occupancy for all the 3d orbitals of $[\text{Fe}(\text{H}_2\text{B}(\text{pz})_2)_2(\text{bipy})]$ for two correlation energies, see Table 1 in supplementary information. We find that the spin-resolved 3d orbital partial occupancy is sensitive to the spin state, but only slightly sensitive to the correlation energy. However, the combined total 3d occupancy is only weakly sensitive to the spin state, and generally insensitive to the correlation energy. The second possibility is that the multiplet splitting and satellite peaks are indicative of spin-state of the films. The multiplet splitting is expected for 2p XPS spectra of iron species with unpaired spins and is absent in the XPS spectra for iron species with paired spins [33, 36, 39-41]. From the observation of multiplet splitting in figure 2(a)(i) follows that the molecules in as deposited bilayer films are in high-spin state at room temperature. The principal

Spin state locking of Fe(II) spin crossover complex

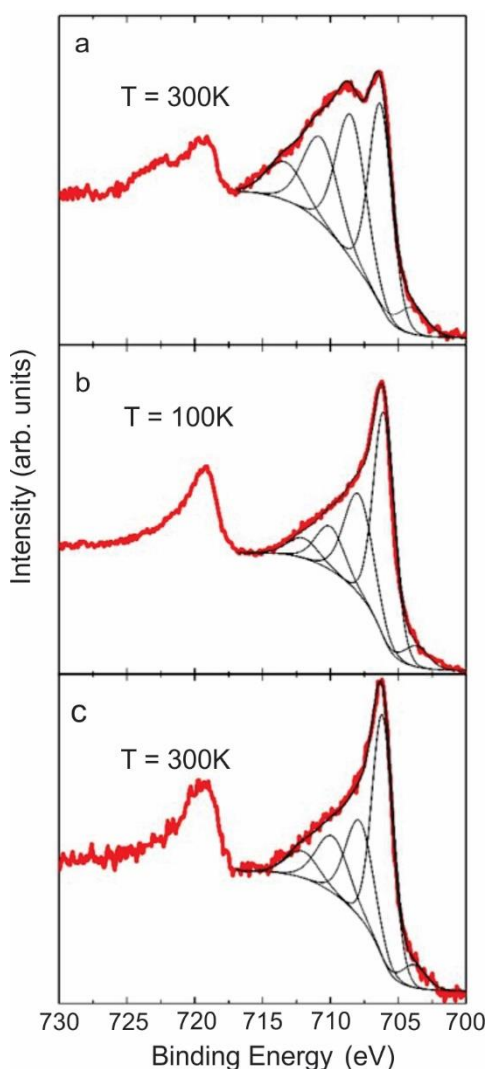


Figure 3. Temperature dependent XPS of a bilayer $[\text{Fe}(\text{H}_2\text{B}(\text{pz})_2)_2(\text{bipy})]$ thin film on Au(111) (a) Fe 2p core level spectra at room temperature for as grown film (b) Fe 2p core level spectra at 100 K (c) Fe 2p core level spectra after heating the sample back to room temperature.

satellite intensity decreases as the film thickness is increased and if the Fe 2p core level satellite features are representative of unpaired spins within $[\text{Fe}(\text{H}_2\text{B}(\text{pz})_2)_2(\text{bipy})]$ then obviously thinner films would have a significantly greater percentage of as-deposited molecules in the high spin state than thicker films. We believe, however, that the multiplet splitting is due to molecule substrate interaction. The closer the proximity to the gold substrate for a molecule within the film, the greater the numbers of unpaired spin multiplets that are

accessed in the photoemission final state. This effect of change in the satellite intensity can be seen in the angle-dependent XPS for 7 ± 3 monolayer film as shown in figure 2(b). As the angle between the sample and analyzer is increased, the principal satellite intensity is reduced. Both thickness and angle dependent data, therefore, suggest that interfacial layers are different from the layers away from the interface. This difference can be due to the molecule-substrate interaction or the packing of the molecules in the films of different thicknesses. To bring some clarity, we have investigated the temperature dependence of the electronic structure of the films, as discussed in the following.

3.3 The Irreversible Locking of the Spin State

Figure 3 shows the change in the Fe 2p XPS spectra of a bilayer $[\text{Fe}(\text{H}_2\text{B}(\text{pz})_2)_2(\text{bipy})]$ thin film with temperature. Again, as in figure 2(a), the Fe 2p core level XPS spectra, taken immediately following molecular film growth at room temperature, show strong satellite contributions, characteristic of unpaired spins in the $[\text{Fe}(\text{H}_2\text{B}(\text{pz})_2)_2(\text{bipy})]$ bilayer film. These satellite features are suppressed in the spectra when the film is cooled to 100 K (figure 3(b)), and do not reappear if the temperature of the sample is increased back to room temperature (figure 3(c)). This irreversible change of the Fe 2p peak, together with the STM images in figures 1(a) and (b), suggest that the reduction in peak splitting is associated with a temperature-induced change in the stacking and possibly the conformation of the interfacial molecules during cooling. It is clearly seen from the STM images at RT and at 77 K that there is a change of the molecular with cooling, in the form of condensation of an apparently disordered and gaseous molecular layer into a bilayer at this coverage. Likely, not only the stacking of the molecule changes at lower temperature, other more subtle changes, not visible in STM images, might also occur during cooling as a result of this rearrangement of the molecules. This could include a distortion of the molecular ligands, and an overall change in molecule-molecule distances. It is thus to be expected that the spin state of the molecules would be affected as well.

The irreversible change in the satellite intensity suggests that some of the molecules show thermal spin transition from the HS state to the LS state when film is cooled but there is no transition back to the HS state when film is warmed back up to the

Spin state locking of Fe(II) spin crossover complex

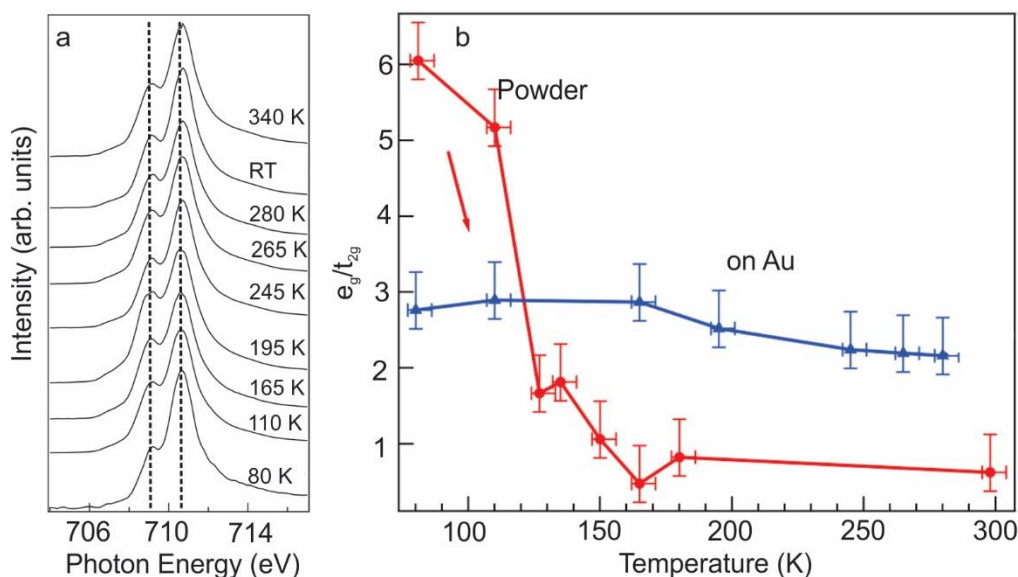


Figure 4. (a) The temperature dependent X-ray absorption spectra of a bilayer $[\text{Fe}(\text{H}_2\text{B}(\text{pz})_2)_2(\text{bipy})]$ film on Au(111) versus temperature, (b) The temperature dependence of the relative empirical unoccupied “ e_g/t_{2g} ” state ratio extracted from XAS for $[\text{Fe}(\text{H}_2\text{B}(\text{pz})_2)_2(\text{bipy})]$ powder (red circles) and ultrathin molecular films on Au(111) (blue triangles). In both cases the data were taken after cooling to below 100 K, then increasing the temperature to the value indicated.

room temperature. Does this mean coexistence of locked high-spin and low-spin states during annealing through the SCO transition temperature? As noted above, it is already known [16, 18] that a conducting substrate, like Au(111), tends to pin more than 50% of several SCO complexes in the high spin state even well below the SCO transition temperature. To investigate this point further, we have utilized X-ray absorption spectroscopy.

The Fe L-edge X-ray absorption (XAS) spectra are representative of resonant state-to-state transitions of electrons from the occupied Fe $2p$ orbital to unoccupied $3d$ orbitals. Other intra-atomic Fe transitions from $2p$ to $4s$ are of low probability, while excitations to $4p$ are dipole forbidden. Figure 4(a) illustrates temperature-induced changes in the XAS features across the spin crossover transition temperature of 80 K to 340 K for $[\text{Fe}(\text{H}_2\text{B}(\text{pz})_2)_2(\text{bipy})]$. Like in prior studies [18], also the XAS spectra of the $[\text{Fe}(\text{H}_2\text{B}(\text{pz})_2)_2(\text{bipy})]$ bilayer film are characteristic of a mixed spin state with significant contributions from both e_g and t_{2g} Fe weighted unoccupied molecular orbitals. The analysis of the XAS data for the $[\text{Fe}(\text{H}_2\text{B}(\text{pz})_2)_2(\text{bipy})]$ powder, following a procedure described in Ref. [47], provides experimental values of the e_g/t_{2g} ratios of 0.7 ± 0.2 for

the high spin state and ~ 5.0 to 5.9 for the low spin state, as seen in figure 4(b). These values are consistent with expectations from theory [47]. The increased sensitivity of the e_g/t_{2g} ratios to the choice of U in the low spin state, lies in the fact that t_{2g} -like orbitals remain mostly occupied in the low spin state whereas e_g is unoccupied. The empirical e_g/t_{2g} ratio extracted from the XAS spectra is particularly sensitive to a modest variation of t_{2g} occupation. By stark contrast, the e_g/t_{2g} ratios of the same molecules as a bilayer film on Au(111) clearly show that the ratio of high-spin to low-spin state varies only slightly with temperature. On this basis, using the XAS powder derived empirical values and applying these values to the XAS bilayer film, our data suggest that the proportion of molecules in the high spin state at low temperatures is $59 \pm 6\%$ and $71 \pm 6\%$ in the high spin state at room temperature. This is nearly identical to the results obtained for submonolayer films on Au(111) [18]. Nonetheless, this seems to contradict the results in figure 3 where the absence of strong contributions from satellite features suggests that the ultrathin molecular film is characteristic of $[\text{Fe}(\text{H}_2\text{B}(\text{pz})_2)_2(\text{bipy})]$ with paired, not unpaired, spins once cooled to low temperatures.

Spin state locking of Fe(II) spin crossover complex

An important consideration in this discussion is that the e_g/t_{2g} ratio in the high spin state is quite insensitive to the choice of the Hubbard U parameter, but in the low spin state the e_g/t_{2g} ratio varies from 3.8 to 5.8 for $3 \text{ eV} \leq U \leq 6 \text{ eV}$, as summarized in figure S2 in the supplementary information. This allows for only two possible conclusions: either the gold substrate stabilizes the molecular SCO thin films in a mixed spin state, which is dominated by the high spin state ($59 \pm 6\%$ to $71 \pm 6\%$), or the gold substrate alters the applicable correlation energy. But if the presence of a Au substrate indeed changes the correlation energy U , say reducing it by a factor of 2 from $U=6 \text{ eV}$ to $U=3 \text{ eV}$, then the XAS spectra of our bilayer $[\text{Fe}(\text{H}_2\text{B}(\text{pz})_2)_2(\text{bipy})]$ films on Au(111) should be representative of a lower fraction of molecules in the high spin state at low temperatures, as little as $32 \pm 6\%$. Meanwhile the fraction of molecules in the high spin state at higher temperatures would have to be reduced to $51 \pm 6\%$.

4. Conclusions

The interaction of the $[\text{Fe}(\text{H}_2\text{B}(\text{pz})_2)_2(\text{bipy})]$ spin crossover complex with Au(111) substrates inhibits the spin crossover transition of the molecules so that there is a relatively fixed ensemble of molecules in both high spin and low spin states preserved over a wide temperature range, including the temperature range across the spin crossover transition temperature of powdered samples. This locking of the spin states does not occur upon adsorption, but rather after quenching to low temperature. It is most likely the result of a conformational change of the interfacial molecules, whereas the Hubbard correlation energy between the molecules does not appear to be affected by the substrate. Molecules in thicker films, above a film thickness > 20 molecular layers, can however reversibly undergo spin crossover and are not impeded by interfacial effects. This study contributes to the current discussion of spin crossover complexes as emerging candidate material for organic spintronics applications by helping establish the role of interfaces in 2D layers of $[\text{Fe}(\text{H}_2\text{B}(\text{pz})_2)_2(\text{bipy})]$ on Au(111) substrate.

Acknowledgements

This research was primarily supported by the National Science Foundation through the Nebraska MRSEC (DMR-1420645). Partial financial support

of the Agence Nationale de la Recherche (MULTISELF 11-BS08-06, Labex NIE 11-LABX-0058_NIE within the Investissement d'Avenir program ANR-10-IDEX-0002-02, CHIOTS 11-JS07-013-01) and the International Center for Frontier Research in Chemistry (icFRC, Strasbourg) are also gratefully acknowledged. Use of the National Synchrotron Light Source, Brookhaven National Laboratory, was supported by the U.S. Department of Energy, Office of Basic Energy Sciences, under Contract No. DE-AC02-98CH10886.

References

- [1] Bousseksou A, Molnár G, Salmon L and Nicolazzi W 2011 *Chem. Soc. Rev.* **40** 3313
- [2] Guionneau P, Létard J-F, Yufit D S, Chasseau D, Bravic G, Goeta A E, Howard J A K and Kahn O 1999 *J. Mater. Chem.* **9** 985
- [3] Gütllich P, Garcia Y and Goodwin H A 2000 *Chem. Soc. Rev.* **29** 419
- [4] Gütllich P and Goodwin H A 2004 *Springer: Berlin* **233** 1
- [5] Halcrow M A, 2011 *Chem. Soc. Rev.* **40** 4119
- [6] Létard J-F, Guionneau P and Goux-Capes L, Gütllich P, Goodwin H A 2004 *Springer: Berlin* **235** 221
- [7] Salmon L, Molnár G, Cobo S, Oulié P, Etienne M, Mahfoud T, Demont P, Eguchi A, Watanabe H, Tanaka K and Bousseksou A 2009 *New J. Chem.* **33** 1283
- [8] Ksenofontov V, Gaspar A B, Levchenko G, Fitzsimmons B, and Gütllich P, 2004 *J. Phys. Chem. B* **108** 7723
- [9] Zhang X, Palamarciuc T, Létard J-F, Rosa P, Lozada E V, Torres F, Rosa L G, Doudin B and Dowben P A 2014 *Chem. Comm.* **50** 2255
- [10] Naggert H, Bannwarth A, Chemnitz S, von Hofe T, Quandt E and Tuczec F 2011 *Dalton Trans.* **40** 6364
- [11] Ohkoshi S, Imoto K, Tsunobuchi Y, Takano S and Tokoro H 2011 *Nature Chemistry* **3** 564
- [12] Bousseksou A, Molnár G, Demont P, and Menegotto J 2003 *J. Mater. Chem.* **13** 2069
- [13] Prins F, Monrabal-Capilla M, Osorio E A, Coronado E and van der Zant H S J 2011 *Adv. Mater.* **23** 1545
- [14] Real J A, Gaspar A B, and Muñoz M C 2005 *Dalton Trans.* 2062
- [15] Sato O, Tao J and Zhang Y Z 2007 *Angew. Chem. Int. Ed.* **46** 2152
- [16] Gopakumar T G, Bernien M, Naggert H, Matino F, Hermanns C F, Bannwarth A, Mühlenberend S, Krüger A, Krüger D,

Spin state locking of Fe(II) spin crossover complex

- Nickel F, Walter W, Berndt R, Kuch W and Tuczek F 2013 *Chem. – Eur. J.* **19** 15702
- [17] Miyamachi T, Gruber M, Davesne V, Bowen M, Boukari S, Joly L, Scheurer F, Rogez G, Yamada T K, Ohresser P, Beaurepaire E and Wulfhökel W 2012 *Nature Comm.* **3** 938
- [18] Warner B, Oberg J C, Gill T G, El Hallak F, Hirjibehedin C F, Serri M, Heutz S, Arrio M-A, Sainctavit P, Mannini M, Poneti G, Sessoli R and Rosa P 2013 *J. Phys. Chem. Lett.* **4** 1546
- [19] Zhang X, Palamarciuc T, Rosa P, Létard J-F, Doudin B, Zhang Z, Wang J and Dowben P A 2012 *J. Phys. Chem. C* **116** 23291
- [20] Rojas G, Chen X, Bravo C, Kim J-H, Kim J-S, Xiao J, Dowben P A, Gao Y, Zeng X C, Choe W, and Enders A 2010 *J. Phys. Chem. C* **114** 9408
- [21] Rojas G, Simpson S, Chen X, Kunkel D A, Nitz J, Xiao J, Dowben P A, Zurek E, and Enders A 2012 *Physical Chemistry Chemical Physics* **14** 4971
- [22] Kunkel D A, Hooper J, Simpson S, Miller D P, Routaboul L, Braunstein P, Doudin B, Beniwal S, Dowben P A, Skomski R, Zurek E, and Enders A 2015 *J. Chem. Phys.* **142** 101921
- [23] Palamarciuc T, Oberg J C, Hallak F E, Hirjibehedin C F, Serri M, Heutz S, Létard J-F and Rosa P 2012 *J. Mater. Chem.* **22** 9690
- [24] CasaXPS Version 2.3.1 1999.
- [25] Repoux M 1992 *Surf. Interface Anal.* **18** 567
- [26] Shirley D A 1972 *Phys. Rev. B* **5** 4709
- [27] <http://www.nsls.bnl.gov/beamlines/beamline.asp?blid=u4b>.
- [28] Blöchl P E 1994 *Phys. Rev. B* **50** 17953
- [29] Kresse G and Hafner J 1993 *Phys. Rev. B* **48** 13115
- [30] Kresse G and Furthmüller J 1996 *Phys. Rev. B* **54** 11169
- [31] Real J A, Muñoz M C, Faus J and Solans X 1997 *Inorg. Chem.* **36** 3008
- [32] Liechtenstein A I, Anisimova V I and Zaanen J 1995 *Phys. Rev. B* **52** R5467
- [33] Pronschinske A, Bruce R C, Lewis G, Chen Y, Calzolari A, Buongiorno-Nardelli M, Shultz D A, Youb W and Dougherty D B 2013 *Chem. Comm.* **49** 10446
- [34] Gopakumar T G, Matino F, Naggert H, Bannwarth A, Tuczek F and Berndt R 2012 *Angew. Chem. Int. Ed.* **51** 6262
- [35] Gupta R P and Sen S K 1974 *Phys. Rev. B* **10** 71
- [36] Grosvenor A P, Kobe B A, Biesinger M C, and McIntyre N S 2004 *Surf. Interface Anal.* **36** 1564
- [37] Cao S, Paudel T R, Sinha K, Jiang X, Wang W, Tsymbal E Y, Xu X, and Dowben P A 2015 *J. Phys. Condens. Matter* **27** 175004
- [38] Gupta R P and Sen S K 1975 *Phys. Rev. B* **12** 15
- [39] Ellingsworth E C, Turner B, and Szulczewski G 2013 *RSC Advances* **3** 3745
- [40] Johansson L Y, Larsson R, Blomquist J, Cederström C, Grapengiesser S, Helgeson U, Moberg L C and Sundbom M 1974 *Chem. Phys. Lett.* **24** 508
- [41] Matienzo L J, Yin L I, Grim S and Swartz W E Jr 1973 *Inorg. Chem.* **12** 2762
- [42] Burger K, Ebel H and Madeja K 1982 *J. Elec. Spec. and Rel. Phen.* **28** 115
- [43] Son J Y, Takubo K, Asakura D, Quilty J W, Mizokawa T, Nakamoto A and Kojima N 2007 *J. Phys. Soc. Jpn.* **76** 084703
- [44] Graat P C J and Somers M A J 1996 *Appl. Surf. Sci.* **100/101** 36
- [45] Lin T-C, Seshadri G and Kelber J A 1997 *Appl. Surf. Sci.* **119** 83
- [46] Yamashita T and Hayes P 2008 *Appl. Surf. Sci.* **254** 2441
- [47] Zhang X, Mu S, Chastanet G, Daro N, Palamarciuc T, Rosa P, Létard J-F, Liu J, Sterbinsky G, Arena D, Etrillard C, Kundys B, Doudin B and Dowben P A, 2015 *J. Phys. Chem. C* **119** 16293